NOVA
SCIENCE PUBLISHERS, INC.

MULTIPLEXING HOLOGRAMS FOR DATA PAGE STORAGE

Elena Fernandez Varó

Manuel Pérez Molina

Rosa Fuentes Rosillo

Celia García Llopis

Augusto Beléndez Vázquez

Inmaculada Pascual Villalobos

400 Oser Avenue, Suite 1600
Hauppauge, N. Y. 11788-3619
Phone (631) 231-7269
Fax (631) 231-8175
E-mail: Main@novapublishers.com
http://www.novapublishers.com

In: "Data Collection and Storage"
Editor: Julian R. Eiras
ISBN: 978-1-61209-689-6 2012

In: Data Collection and Storage
Editor: Julian R. Eiras
ISBN 978-1-61209-689-6

Chapter 2

MULTIPLEXING HOLOGRAMS FOR DATA PAGE STORAGE

Elena Fernandez Varó[1], Manuel Pérez Molina[2], Rosa Fuentes Rosillo[1], Celia García Llopis[1], Augusto Beléndez Vázquez[2], and Inmaculada Pascual Villalobos[1]

[1] Dep. Óptica, Farmacología y Anatomía, Universidad de Alicante, Spain
[2] Dep. Física, Ingeniería de Sistemas y Teoría de la Señal, Universidad de Alicante, Spain

ABSTRACT

We live in an age of information science and new technologies in which the use of computers, music players, and video or data storage memory for information processing and storage has become essential. The conventional optical memory technologies, like CD-ROMs and DVDs, are two-dimensional surface-storage techniques, and thus have almost arrived at the limit of their capacity and are becoming obsolete. This fact has given rise to many researchers in the world focusing on new techniques to design devices with larger storage capacity such as holographic storage devices. These devices can store the entire volume of the informational material thereby increasing storage capacity compared with 2D that can only store the information on the surface.

In order to manufacture a holographic data storage device it is necessary to get the maximum number of holograms in the recording material. Therefore, it is necessary to study the different techniques that allow multiplexing a large number of holograms on the material. The information to be stored is introduced through liquid crystal displays, (LCD). These devices have been extensively studied for use as spatial light modulators (SLM) due to their ability to modify, in real time, both the amplitude and phase of the incident light. In particular, data pages are sent to the LCD and their spatial frequencies are recorded in the material.

Binary intensity modulation is commonly used to encrypt the information sent to the LCD. However, this type of modulation produces a high zero frequency with an intensity several orders of magnitude higher than other frequencies. As a result, the dynamic range of the material is saturated, limiting the storage capacity.

The problems caused by the lack of homogeneity at the spectrum can be solved by using some other modulation schemes, such as random phase masks, binary π radians phase-only modulation (πBPM), full multi-phase scheme or hybrid ternary modulation (HTM).

The study proposed in this abstract combines the basic elements needed for a realistic realization of a holographic data storage system: the recording material, the codification scheme for the data pages, and the multiplexing methodology.

INTRODUCTION

We live in the age of information science and new technologies, in which the use of computers music players, video, and data storage memory for information processing and storage has become something quotidian. The users of these technologies store large amounts of digital data. In addition, huge amounts of data on the banks, companies, or government archives are stored on devices that occupy a large space, which could be reduced if the devices had a higher storage capacity per unit volume. Conventional optical memory technologies like CD-ROMs and DVDs are two-dimensional surface-storage techniques, and thus they have almost reached the limit of their capacity and become obsolete. This fact has encouraged world researchers to focus on new techniques to design devices with larger storage capacity, as it is the case of holographic storage devices. These devices can store the entire volume of the informational material thereby increasing the storage capacity in comparison with two-dimensional devices that only store the information on the surface. Companies such as Bayer and InPhase came together to create the Tapestry™ [1,2], the first prototype of a holographic optical storage system that is being used by leading companies and is capable of storing 200 Gbytes to 1.6 Tbytes in a disk 130 mm of diameter.

The manufacture of a holographic data storage device requires getting the maximum number of holograms in a recording material, so it is necessary to study the different techniques that allow multiplexing a large number of holograms on the material. The information to be stored is introduced through Liquid Crystal Displays (LCD) [3-6], which have been extensively studied to be used as spatial light modulators (SLM) for their ability to modify in real time the amplitude and phase of the incident light. In particular, data pages are sent to the LCD and their spatial frequencies are recorded in the material, commonly using binary intensity modulation to encrypt the information sent to the LCD. However, this type of modulation gives rise to a high peak at zero frequency (d. c. component) whose intensity is several orders of magnitude higher than the rest of frequencies [7]. Because of this zero frequency peak, the dynamic range of the material is saturated and therefore the storage capacity is constrained.

The problems caused by the lack of homogeneity in the spectrum can be solved by using other modulation schemes different to the binary one, such as random phase masks [8], binary π radians phase-only modulation (πBPM) [9-12], full multi-phase scheme [13,14] or hybrid ternary modulation (HTM) [10,12,15-17]. The study proposed in this chapter combines the basic elements required for a realistic fabrication of a holographic data storage system: the recording material, the codification scheme for the data pages and the multiplexing methodology.

1. Holographic Multiplexing Gratings

To manufacture holographic memory considerations must be taken into account to achieve the maximum storage capacity of digital information. The first consideration is the storage of multiple gratings, which requires suitable materials with high storage capacity. These materials must have large thickness (about 1 mm), high sensitivity, and their selectivity angular energy must be as small as possible, thereby allowing them to obtain high values for the dynamic range [18]. The second consideration is the amount of stored information, which is the maximum number of bits/μm^2. In this sense, it is necessary to use the holographic multiplexing techniques that allow storage of the largest number of holograms in the same position of the material [19-

21]. Thirdly, all the holograms to be stored must have the same diffraction efficiency, which is needed to better exploit the dynamic range of the material and to store more holograms achieving higher diffraction efficiencies. For this reason, we will use a recording method to calculate the exposure time for each of the holograms to achieve equal diffraction efficiencies [22].

1.1. Experimental Setup

The experimental setup used for recording holographic diffraction gratings is shown in Figure 1. The laser used in the recording stage is an Nd: YVO4 (Coherent Verdi V2) that emits a beam of light with a wavelength of 532 nm, at which the material is sensitive. The laser used in the reconstruction stage is a He-Ne laser at 633 nm, wavelength at which the material is not sensitive.

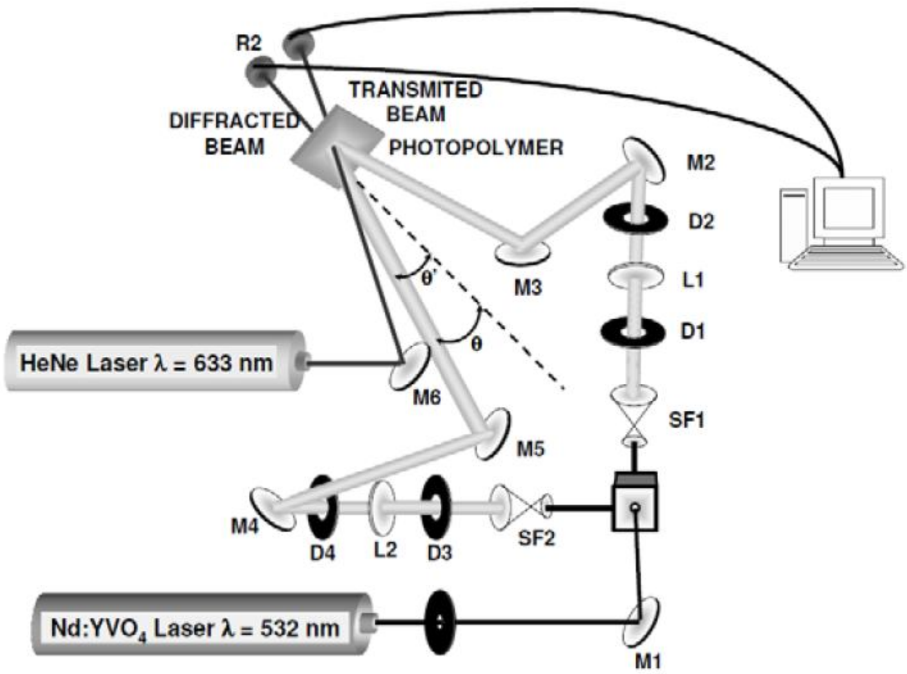

Figure 1. Holographic Setup. Me: mirrors, BS: beam splitter, Li: lens, SFi: A set of spatial filter and microscope objective, Di: diaphragm, Ri: radiometers.

In the registration stage, two coherent beams named object beam and reference beam overlap in the material to form the hologram (in this section both beams will be regarded as plane waves, so the resulting interference pattern will be a diffraction grating). These two beams are the result of splitting the beam emitted by the laser by means of a beam splitter, and each of them passes through a microscope objective and a pinhole to be expanded and filtered respectively. Then each beam passes through a series of lenses and diaphragms that collimate them with the desired diameter, and finally, the beams are directed to the material with the desired angle through a series of mirrors.

1.2. Multiplexing Methods

The hologram multiplexing consists of storing multiple holograms without overlapping in a given position of the material. The best way to optimize the entire volume of the holographic material is to combine different methods to store all multiplexed holograms allowed by the material avoiding the overlapping between different holograms. Different hologram multiplexing methods can be found in the literature [23]:

a) Angular multiplexing in plane: The reference beam is a plane wave and the multiplexing occurs when varying the angle of incidence of reference beam, being the latter is always in the same plane as the object beam [24].
b) Angular multiplexing out of plane: It is similar to the previous method, but here the reference beam is in the plane normal to the optical axis defined by the object beam.
c) Peristrophic multiplexing: The reference beam is a plane wave, and the object and reference beams overlap on the material forming a certain angle. The multiplexing occurs when spinning the material with respect to a rotation axis perpendicular [22,25] or parallel [18,19,26] to its surface.
d) Wavelength multiplexing: The reference beam is a plane wave and the multiplexing mechanism is the change in the wavelength of the reference beam [22,27,28].
e) Phase code multiplexing: The reference beam is a plane wave modulated in one dimension by a spatial light modulator. The dimension that is modulated is the plane defined by the optical axis of the object beam and the reference beam [8].
f) Shift multiplexing in plane: The reference beam is a spherical wave and the mechanism of multiplexing is based on the location of holographic media with respect to the reference beam. [29].

g) Shift multiplexing out of plane: The reference beam is a spherical wave that is in the plane normal to the optical axis defined by the object beam and its projection on the surface of the recording material.
h) Spatial multiplexing: The object and reference beams impinge on the material in different spatial positions for the different holograms.

1.3. Recording Material

The main feature of a good holographic recording material is the ability to modify some of its optical properties, such as the absorption coefficient, the thickness or the refractive index [30] by exposing it to light, preferably with a linear response for the previous properties with respect to light exposure. In addition, these materials must have a high resolution, since the separation between the interference fringes is usually of the order of 1 μm or less. Another aspect to be considered is the range of wavelengths absorbed by the material, since the recording wavelength of the laser must lie within this range so that hologram recording is achievable. In addition, these materials must also have high-energy sensitivity, low noise, low absorption losses, stability during the recording of hologram and, they must be reusable and/or as cheap as possible.

Different types of recording material with some the aforementioned properties have been investigated, as in the case of photographic emulsions, photochromic materials, the photoresist, photothermoplastic materials, dichromated gelatin, gelatin silver halide sensitized, photopolymers, and photorefractive materials. Recently, many studies have focused on the manufacture and optimization of materials that can be used for holographic storage. Such materials can be either single-use (WORM, write one, read many) [18,31-36] or rewritable [36-38]. In addition, biodegradable materials are also being currently studied [39,40].

However, amongst these materials, we can highlight the photopolymer as the most versatile for several reasons: they allow the storage of holograms with high refractive index modulation and high optical quality, do not require development processes, have a low cost, and can easily vary their properties (such as energy sensitivity or spectral absorption rate) by simply changing its composition [18,31,41]. Besides, these materials can exhibit a high dynamic range depending on their thickness. The dynamic range M # is a parameter that describes the ability of a material, together with the experimental device, to store holograms [19,31,42]. In order to store the maximum amount of information in a holographic memory, the dynamic range is required to be as high as possible so that one can store the largest number of holograms in the same position and with the highest diffraction performance.

1.4. Angular Selectivity

An important parameter that must be measured is the angular selectivity of the holographic material, which defines the minimum angular separation distance between the holograms so that they do not overlap. In this chapter, the holograms are recorded using peristrophic multiplexing with respect to two rotation axes, one of them perpendicular to the material surface and the other one parallel to it, so the angular selectivity will be calculated with respect to both axes.

In the case of perpendicular peristrophic multiplexing, the method used to calculate the angular selectivity is described in references [23,25]. Because of the geometry of this type of multiplexing, in the reconstruction stage of one of the holograms, the diffracted beams from the rest of holograms also appear, but they are reconstructed at different angles. Consequently, the problem of measuring the angular selectivity reduces to calculate the angular size of the detector surface wherever it is placed and ensure that the holograms are stored with an angular separation greater than the angular size of the detector. The main advantage of perpendicular peristrophic multiplexing is that the calculation of the angular selectivity is purely geometrical and it can be modified by changing the size of the detector or the distance between the detector and the hologram.

In the case of parallel peristrophic multiplexing [43,44], the angular selectivity is defined as the angular bandwidth of the main lobe of the diffraction efficiency curve when it is plotted as a function of the reconstruction angle. In order to store multiple holograms without overlapping, it is necessary to measure the angular bandwidth of the main lobes for the different holograms to make sure that the angular spacing between such lobes is greater than their angular bandwidth. This kind of study achieves the maximum number of angular recording positions without overlapping in any of the holograms.

1.5. Dynamic Range

Another important parameter in the design of holographic data storage memories is the dynamic range [19,31,42]. The dynamic range is defined as the number of holograms with a diffraction efficiency $\eta = 1$ (100%) that can be stored in a material with a given thickness. Its mathematical expression is given by:

$$M\# = \sum_{i=1}^{N} \eta_i^{1/2} \tag{1}$$

where η_i is the diffraction efficiency of each hologram, and N the number of recorded holograms.

To calculate the dynamic range we must sum the square roots of the diffraction efficiencies of all the holograms that have been recorded in the material, as it is shown in equation 1. From the dynamic range, it is possible to find out the number of holograms that could be stored in the material to obtain a certain diffraction efficiency or alternatively the average diffraction efficiency for a given number of stored holograms. This latter average efficiency is given by:

$$\eta_{AVR} = \left(\frac{M\#}{N}\right)^2 \tag{2}$$

where N is the number of stored holograms.

1.6. Holographic Storage of Diffraction Gratings

Once the energy sensitivity of the material [45], the angular selectivity and dynamic range are defined, the next step is to store the diffraction gratings in the material. It is recommended that all holograms be stored with the same diffraction efficiency in order to avoid errors that may appear in the reading of the hologram because of too low diffraction efficiencies or due to the fact that the dynamic range is not distributed along all the holograms. For this purpose, the holograms are stored with uniform diffraction efficiencies by using the Schedule Exposure Method (SEM). This method calculates the optimal exposure times to make uniform the diffraction performance of all holograms, taking into account the diffraction efficiencies obtained by storing a number of holograms.

To fully exploit the dynamic range of the material it is necessary to store as many holograms as possible. In this study, 90 holograms are stored at the same location using a combination of perpendicular and parallel peristrophic multiplexing [46].

For the first hologram to be recorded, a specific exposure must be used taking into account that the material will not respond under lower exposures. For this reason, the first hologram is stored with an exposure time of 2 seconds. In order to store the other holograms, different configurations were tested previously. First, we stored all the holograms with the same exposure time, but the first holograms had high diffraction efficiencies and the last ones had diffraction efficiencies close to 0%. When the holograms are stored, the monomer and the dye are consumed and therefore the material becomes less sensitive. For this reason, it is necessary to increase the exposure time for the last holograms so that they reach the same diffraction efficiency as the first ones. Instead of storing all the holograms with the same exposure time, we decided to increase this time as the number of stored holograms increased. The exposure times that are used initially to store the holograms and that are chosen depending on the material are called "initial iteration times" in our study.

The exposure time used to store the holograms at the initial iteration is given as follows: 2 s for the first hologram (necessary time so that the material responds), 0.5 s for holograms 2 to 6, and for every additional five stored holograms we add 0.5 s [47]. Once the holograms have been stored with the exposure times of the initial iteration, the diffraction efficiency of each one of them is measured. Figure 2 represents with full circles the diffraction efficiency obtained with these exposure times, and it can be appreciated that the first holograms exhibit higher diffraction efficiency (around 2.5%) than the last holograms (around 0.02%). Therefore, for the holograms to be stored with uniform diffraction efficiency it is necessary to decrease the exposure times for the first holograms and increase the exposure times for the last ones. The SEM is used to calculate these exposure times, which are called "exposure times of first iteration".

From the diffraction efficiencies given in Figure 2, we calculated the cumulative grating strength,

$$\sum_{i=1}^{N} \eta_i^{1/2},$$

where η is the diffraction efficiency and N is the number of holograms stored so far. When the curve is saturated, we can obtain the dynamic range, which in this case is M# = 13.5.

In order to store our desired number of 90 holograms with uniform diffraction efficiency, the data obtained from Figure 2 are fitted according to the following theoretical equation:

$$A = a_0 + a_1E + a_2E^2 + a_3E^3 + a_4E^4 + a_5E^5 + a_6E^6 \quad (3)$$

where A is the cumulative grating strength and E the exposure energy. Once the coefficients a_i have been calculated, the time needed to record the holograms may be calculated from equation 4:

$$t_n = A_{Sat} \Big/ N \cdot I \left[a_1 + 2a_2 \sum_{i=1}^{n-1} E_i + 3a_3 \left(\sum_{i=1}^{n-1} E_i \right)^2 + 4a_4 \left(\sum_{i=1}^{n-1} E_i \right)^3 + 5a_5 \left(\sum_{i=1}^{n-1} E_i \right)^4 + 6a_6 \left(\sum_{i=1}^{n-1} E_i \right)^5 \right] \quad (4)$$

where A_{sat} is the obtained dynamic range, N is the number of holograms to be stored, I is the recording intensity, and E_i is the energy used to record up to the i-th hologram.

Figure 2 shows the exposures of the first iteration with empty triangles, which are obtained by fitting the cumulative grating strength according to equations 3 and 4. With these exposures, 90 holograms are stored again and the obtained diffraction efficiency obtained is depicted with empty squares in Figure 2.

After the first iteration, the obtained dynamic range is M# = 12, the mean diffraction efficiency is 2.1% and the diffraction efficiencies are much more uniform and closer to the average diffraction efficiency than the ones obtained with the initial iteration.

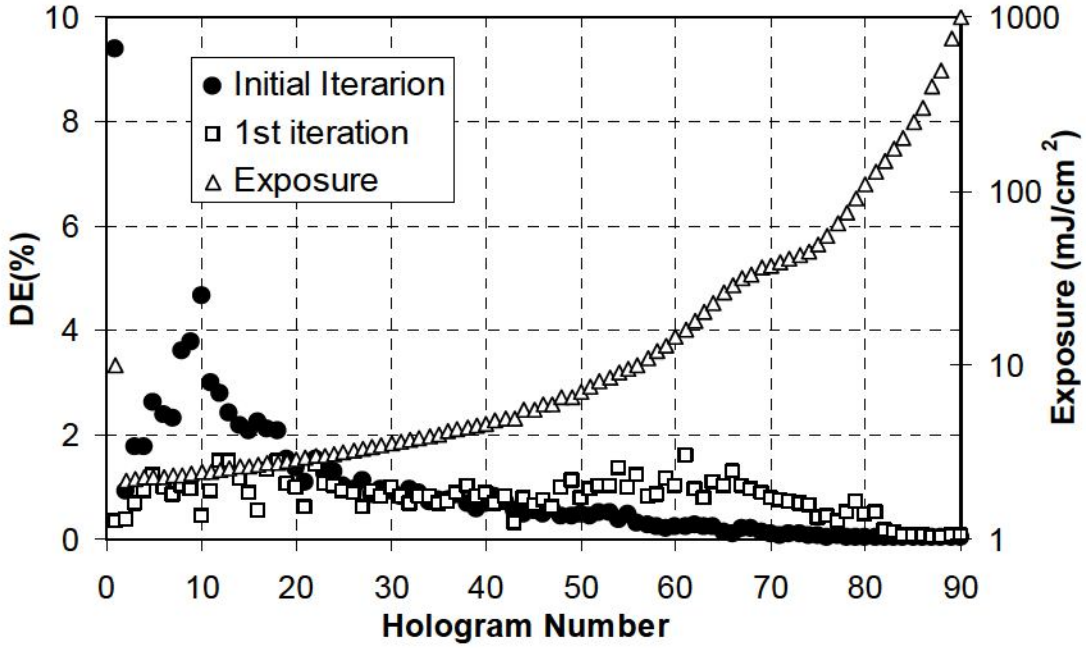

Figure 2. Diffraction efficiency versus hologram number for the initial iteration (full circles) and for the first iteration (empty squares) for a combination of peristrophic and angular multiplexing, and the exposure used to obtain them (empty triangles).

2. Twisted-Nematic Liquid Crystal Displays for Holographic Data Storage

In the previous section, we considered the multiplexing of a large number of gratings, which is the first step to make a holographic storage memory. However, we need to store the information in a digital format made up of bits of information, so the next step is to replace the diffraction gratings by digital data pages that act as an object. The type of object used as a data page is composed of black and white squares to emulate the bits "one" and "zero" respectively. An LCD is used to send such binary objects to the object beam.

We must bear in mind that there are different ways of sending data pages to an LCD, that is, there are different ways to modulate the object beam in the holographic setup (which is what is stored in the material). Among the different modulations, the binary intensity modulation is one of the most frequently used due to its simplicity. In this type of modulation, the Fourier Transform (FT) of the data page is holographically recorded on a photosensitive material. However, this modulation gives rise to a large zero frequency peak, which may saturate the dynamic range of the material and thus limit the accessible dynamic range. The problems caused by the lack of homogeneity of the FT can be solved by using other different modulation schemes such as random phase masks [8], binary π radians phase-only modulation (πBPM) [9-12], full multi-phase scheme [13,14] or hybrid ternary modulation (HTM) [10,12,15-17].

In this section, we are going to describe how data pages were sent to the LCD and stored in the material using two different types of modulations: binary intensity modulation and hybrid ternary modulation. The main reason we use these two modulations is that we began our study using the binary intensity modulation and then we changed to the HTM because it allowed us to reduce the zero frequency peak using exactly the same experimental scheme as the one for the binary intensity modulation. This interesting feature of the HTM enabled us to compare the results of both modulations. The only difference between binary intensity modulation and the HTM is the type of codified object sent to the LCD, without any additional adjustments in the setup, which makes straightforward the implementation of this new scheme. In this sense, the use of other modulation schemes, such as full multi-phase modulation, involve interferometric methods in the reconstruction, which adds additional complexity to the experimental setup.

In the first step of our holographic recording process, the LCD together with a range of external elements of polarization (polarizers and retardation plate) are calibrated by changing the angle of the external elements of polarization to enable the LCD to behave as desired under certain constraints: as a light amplitude modulator, as a light phase modulator only, etc. Secondly, we optimize the LCD to obtain the suitable angles of the polarizers and retardation plate as well as the gray levels in order to carry out these two types of modulations. Finally, we compare the results obtained with the binary intensity modulation and HTM to see which of them would provide the best for the holographic data storage.

2.1. Characterization of the Spatial Light Modulator

Twisted-nematic liquid crystal displays (TN-LCDs) have been studied for their applications as spatial light modulators (SLMs), which are used to modify in real time the amplitude or phase of a light beam [3-6,17,48]. Some of the most important applications of the LCD are the design of programmable optical elements such as lenses [49] and diffraction gratings, as well as their applications for holographic data storage. In the case of holographic data storage, LCD can refresh the data page to be stored in the material in real time [50].

The LCD changes the polarization state of incident light. In order to control the polarization state at the output of LCD using it as an SLM, it is necessary to place the LCD between linear polarizers and, in general, it is necessary to include a retardant wave plate for calibration purposes [51]. Once the LCD is calibrated, it can modulate the light amplitude and/or phase as desired (with certain constraints) just by changing the angle of the external polarization elements. To achieve the aforementioned modes of operation for the LCD, it is necessary to calibrate the LCD and the polarizers and use the values obtained from the calibration to optimize the external elements and the LCD. This optimization consists of calculating the values of the angles that must be set in the external elements to achieve the desired polarization states. Extensive literature explaining LCD calibration and optimization has been written [4,6,51], so here we will provide with a brief explanation regarding the calibration process.

The calibration process consists of two steps. In the first step, the LCD is turned off and no voltage is applied. In this step, three parameters that are independent of the voltage are calculated: the total twist angle (α), the orientation of the molecular director at the input face (Ψ_D) and the maximum birefringence ($\beta_{max} = \pi d(n_e - n_o)/\lambda$, where d is the thickness of the LCD, n_e is the extraordinary refractive index, n_o is the ordinary refractive index and λ is the wavelength) [52,53]. In the second step, the parameters that depend on the voltage are measured. Such parameters are related to the variation of optical anisotropy properties throughout the thickness of the cell as a function of the applied voltage. This model attempts to take into account the fact that the liquid crystal molecules near the glass are almost completely adhered to its surface and cannot reorient themselves when the voltage is applied. Thus, the total thickness d of the LCD may be decomposed into two lateral regions of width d_1 and a central region of width d_2. In this way, the anisotropic properties of the LCD may be modelled using two voltage-dependent parameters – birefringence β and δ –, which can be expressed as:

$$\begin{aligned} \beta(V) &= \pi \Delta n\, d_2 / \lambda_0 \\ \delta(V) &= \pi \Delta n_{max} d_1 / \lambda_0 \end{aligned} \tag{5}$$

where λ_0 is the beam wavelength, Δn is the difference between the ordinary and extraordinary index and Δn_{max} is the maximum value of Δn.

From the curves $\beta(V)$ and $\delta(V)$ we can find the angles at which the polarizers must be set in the experimental setup to modulate the incident beam. Depending on how the modulator is intended to act (intensity, phase or both), it will be necessary to set some different angles on these polarizers.

2.2. Optimization of the SLM to Obtain Modulations for Holographic Data Storage

Once the LCD is calibrated, the next step is its optimization. The optimization process consists of finding out the gray level values that must be sent to the LCD and the angles of the polarizers, which must be placed before and after the LCD to module the object beam, based on the calibrated birefringence and as a function of voltage applied to the LCD.

For binary intensity modulation it is necessary to find two states which meet the condition of maximum contrast, that is, a state with maximum intensity (white bits of the data page) and another one with low intensity (black bits). Once the adjustment is completed, Figure 3 shows the obtained transmittance values versus the gray level. These values have been obtained for an orientation of the transmission axes of the polarizers given by the angles φ_1=116° and φ_2=111° with respect to the laboratory reference system, where φ_1 corresponds to the polarizer placed in front of the LCD and φ_2 corresponds to the polarizer placed behind the LCD [6]. It has been found that the gray level that provides maximum transmittance is 250, whereas the gray level that provides the lowest transmittance is 0. With these two states, the system achieves a maximum contrast of 98%, where the contrast M is defined as $M = (I_{\max} - I_{\min})/(I_{\max} + I_{\min})$.

This is one of the modulation types that can be used for holographic data storage [54]. However, if the Fourier Transform (FT) is analyzed, we find that the zero order of the FT is several orders of magnitude more intense than the rest of frequencies, which does not help to optimize the dynamic range of the material or imply that the image quality is better. Consequently, this type of modulation would not be the most suitable for holographic data storage, since the zero order consumes the components of the material more quickly, limiting the number of holograms that can be stored.

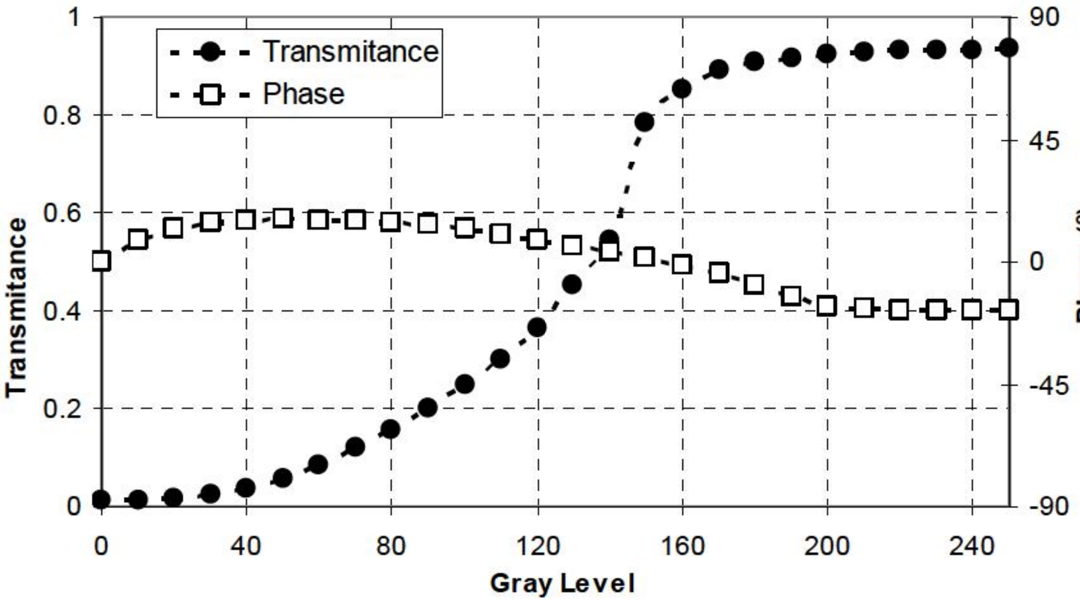

Figure 3. Transmittance and phase obtained in the optimization of the LCD to get a binary intensity modulation.

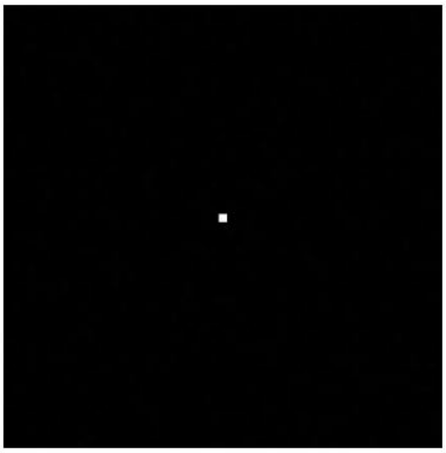

Figure 4. FT obtained with binary intensity modulation.

Figure 4 shows the FT of the data page obtained with the binary intensity modulation. The central area of the FT has been zoomed to appreciate it better. As shown, all the energy is concentrated in the FT zero order and no energy at other frequency components can be observed.

To prevent the zero-order to be so intense (which reduces the storage capacity of the material), people use other types of modulation that allow distributing the intensity among the other frequencies.

Some studies have chosen to blur the FT so that the zero order is not as intense compared to other frequencies, but this procedure is incompatible with the associative property of holographic memories. An alternative option is to use random phase masks to reduce the zero order [8]. Other methods to reduce the zero order consist of the use of a binary phase only modulation where the two states have a phase difference of π rad (πBPM) [7,9,11], or a method that combines the two types of modulation: hybrid ternary modulation amplitude and phase HTM [7,15-17].

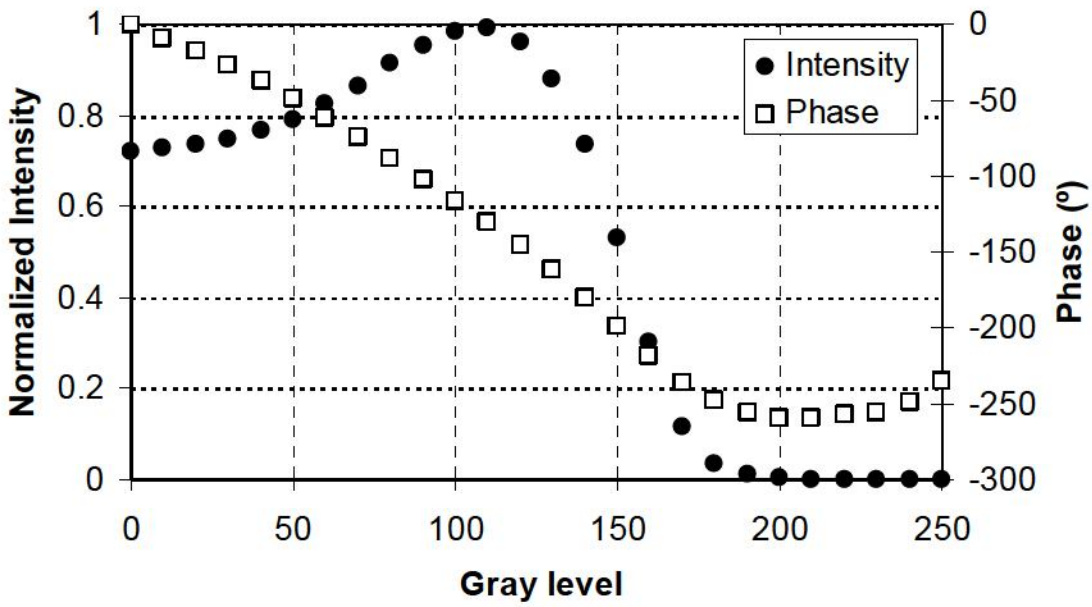

Figure 5. Transmittance and phase obtained in the optimization of the LCD to get the HTM.

In the case of HTM, it is necessary to find three states: two of them corresponding to the white bits with a phase difference of π rad and maximum transmittance, and a third state which corresponds to the black bits with minimum transmittance. After performing the optimization process [6], the obtained transmittance and phase are shown in Figure 5, whose values have been achieved by setting the polarizers at the angles φ_1=134° and φ_2=65°. In this configuration, the two states of maximum transmittance and phase shift of 180 ° is obtained with the gray levels 0 and 140, while the state of minimum transmittance is obtained with the gray level 250. For these gray levels, the maximum contrast is 99% and the phase difference between the two states is 180°.

Figure 6 shows the FT that is obtained by sending an object generated with the three states required in the HTM and the bits chosen randomly. As it can be appreciated, all the frequencies are distributed across the Fourier plane.

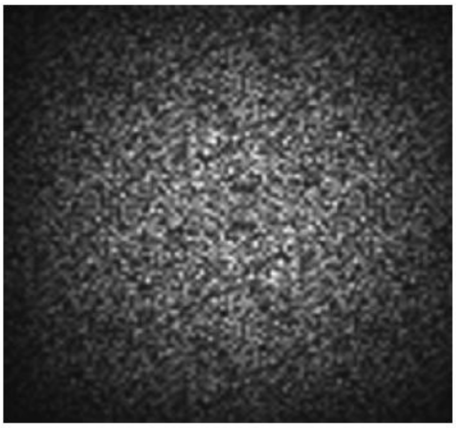

Figure 6. FT obtained with the HTM.

We can therefore conclude that the best modulation to manufacture holographic data memories is the HTM, since it gives a more uniform FT spectrum and thus allows better exploitation of the dynamic range of the holographic material.

2.3. Holographic Setup

In our experimental setup shown in Figure 7, the holographic data pages were stored using a Nd:$YV0_4$ laser (Coherent Verdi V2) with a wavelength of 532 nm, at which the material is sensitive. The polarized beam emitted by the laser was split into two beams with a beam-splitter. Each beam was expanded and filtered using a microscope objective and a pinhole. Then the beams passed through a series of lenses and diaphragms in order to obtain collimated beams with the desired diameter. The two laser beams were spatially overlapped at the recording medium.

The LCD was placed in the object beam between two polarizers and two quarter-wave plates, one in each side of the LCD. The LCD, polarizers, and quarter-wave plates were used as an SLM. In addition, a lens (L4) was placed in front of the SLM to perform the Fourier Transform (FT) of the data page, which was sent to the SLM.

A diaphragm is placed just in front of the photopolymer to block all the diffraction orders that emerge from the LCD except the central order. If the other orders were not blocked, then they would also be stored in the material and interference patterns would be observed on the image during reconstruction, thus worsening the image quality. The reference beam is a plane wave that interferes with the object beam at the material surface. In previous papers we studied how the beam ratio between the object and reference beams affects the quality of the stored images [55]. These beam intensities were measured at the position where the photopolymer must be placed when the holograms are stored.

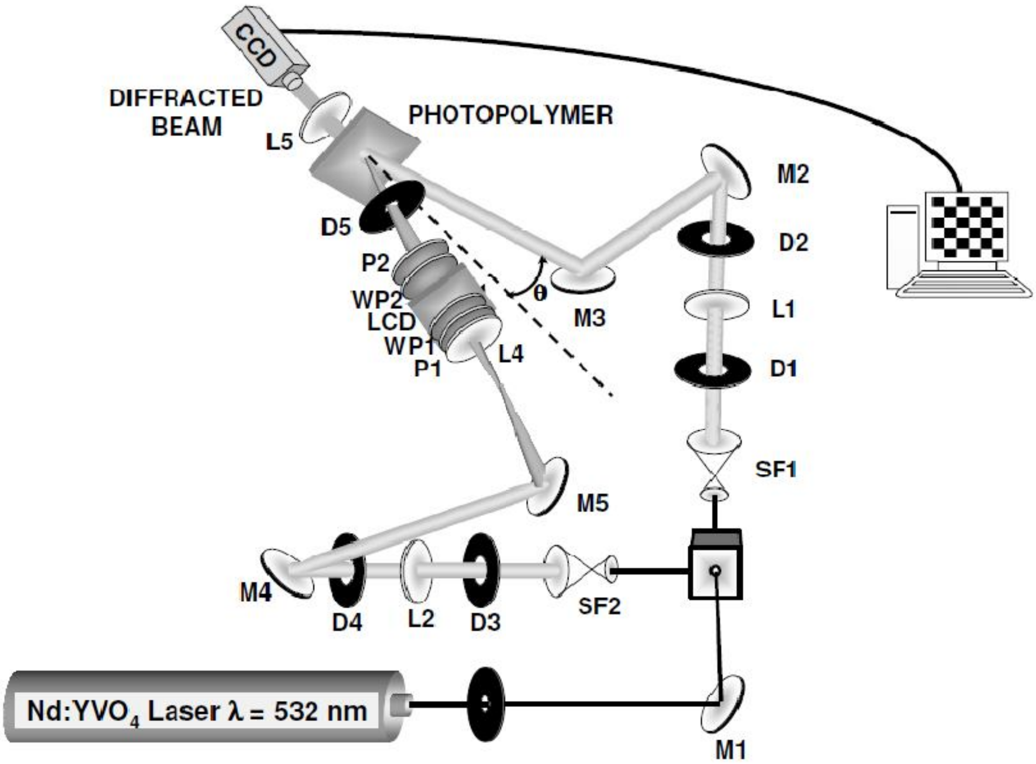

Figure 7. Experimental setup: BS beam splitter, Mi mirror, Li lens, Di, diaphragm, SFi, microscope objective lens and pinhole, SLM spatial light modulator, Pi polarizer, WPi quarter wave plate, CCD charge coupled device.

In the reconstruction stage, once the object has been stored, the hologram is illuminated with the same reference beam used in the recording stage but with a very low intensity in order not to deform the hologram (since the material is sensitive to this wavelength) [3]. Another lens (L5) was placed behind the photopolymer to perform the optical inverse Fourier transform (IFT) of the diffracted beam on the surface of the charge-coupled device (CCD). A computer sent the data pages to the LCD and another computer acquired the images reconstructed by the CCD. This holographic setup will be used to store data pages in the material, using the two modulations described before.

2.4. Bit Error Rate

After one of the objects has been stored in the material, the hologram is reconstructed by illuminating it with the reference beam, and the obtained diffracted beam is imaged onto the CCD. If the holographic reconstruction had been perfect, the obtained images would have had white and black uniform pixels. However, the white and black regions usually have a large number of gray levels, which distort the image. For this reason, it is convenient to measure the Bit Error Rate (BER), which is a parameter that quantifies the image quality. The BER is defined as the probability of having erroneous bits in the image. To calculate the BER [23], first we must represent the probability density of obtaining a certain gray level in the region corresponding to the black and to the white [54,55]. These two probability densities are clearly distinguishable for low BER values, although there is a point at which they intersect. This intersection point of both distributions is called x_c.

Once the probability densities have been obtained, both distributions are fitted to a certain known type probability density. In this study, they are fitted to a Gaussian probability distribution given by:

$$W(x_0, \sigma; x) = \frac{1}{\sqrt{2\pi\sigma}} \exp\left(-\frac{(x - x_0)^2}{2\sigma^2} \right) \tag{6}$$

where x represents each gray level in the image, x_0 the point at which the Gaussian distribution is centred (the mean) and σ the width of the Gaussian distribution (the standard deviation). The reason why the previous distributions are fitted to a Gaussian equation is that it has been verified that most probability distributions obtained from an image captured by a CCD may be expected to follow this type of distribution.

Once the adjustments for the probability densities of both white and black pixels have been carried out, the BER is calculated as:

$$BER = \frac{1}{2}\left[\int_0^{x_c} W_W(x)\,dx + \int_{x_c}^{\infty} W_B(x)\,dx \right] \tag{7}$$

where W_W and W_B are the adjustments of the probability densities for the white and black pixels respectively, and x_c is the point of intersection of the two probability densities. Using this algorithm, the BER of all the images shall be calculated and discussed in the following sections.

2.5. Binary Intensity Modulation and Hybrid Ternary Modulation for Holographic Data Storage

In this section we are going to multiplex four data pages of different bit sizes in a photopolymer plate with a thickness of 500 μm, an angular separation of 3° and a beam ratio R = 100. Once it is stored, it will rebuild with an intensity I_R=0.3mW/cm^2 by capturing the image obtained with a CCD camera. In previous studies it was found that these were the most suitable parameters to get the best image quality [55]. To store as many holograms as possible in the photopolymer, the exposure is increased gradually for the successive holograms so that the latest holograms have the same diffraction efficiency as the initial ones. When all the holograms are stored, they are reconstructed at the end of the registration process with the reference beam, and the diffracted images are captured with a CCD. The BER is then calculated from these images [23,54,55]. This storage process will be carried out for both the binary modulation in intensity and the HTM.

First, data pages are stored using the binary intensity modulation. Figure 8 depicts with empty triangles the exposure for which the holograms will be stored using this modulation. The first object to be stored has a size of 300x300 bits, and its BER is depicted with full circles in Figure 8. For this object, 58 holograms are achieved with a BER below 0.2. In other studies, it has been shown that BER values below 0.2 provide good image quality. For this reason, in this work we consider that the BER values lower than 0.2 are those that provide the best quality images. The holograms 1 to 50 have been stored with a BER value of 0.02. From hologram 51, the BER values increase but remain below 0.2. Then the object of 400x400 bits is stored, and its BER is depicted with empty circles in Figure 8. In this case, 39 holograms are stored with BER values below 0.2. The next object to store has a size of 500x500 bits and it is depicted with full squares in figure 8. In this case, 42 holograms are stored with a BER below 0.2. Finally, we have multiplexed an object of 800x600 bits, whose BER values are depicted with empty squares. As can be appreciated, 53 holograms have been stored with a BER below 0.2.

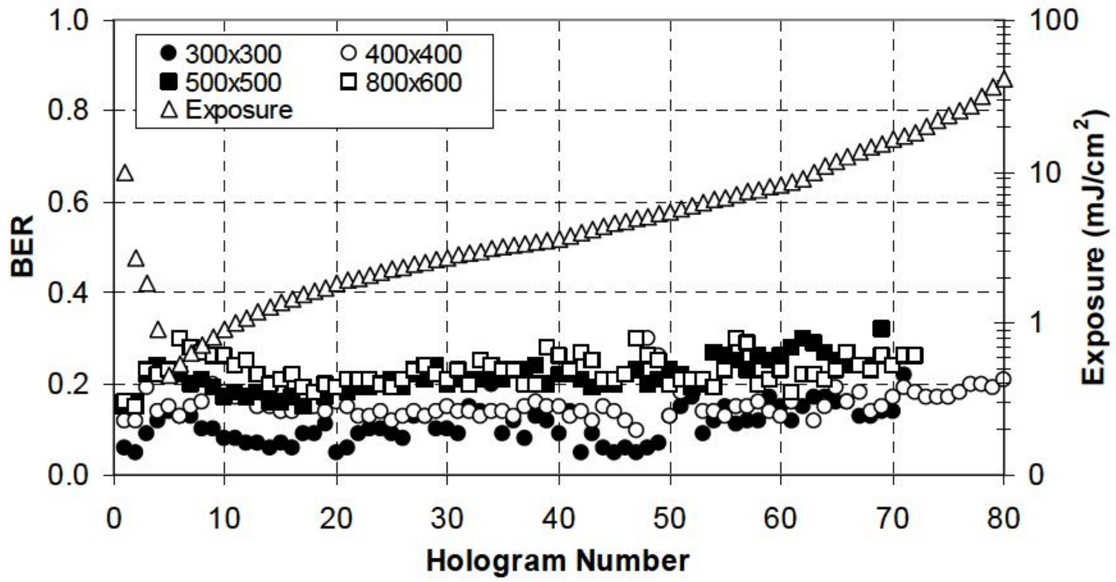

Figure 8. BER of the objects, in a 500 μm thickness material.

Second, the four objects are stored using the HTM to modulate the object beam [56]. The exposure used for storage is depicted with empty triangles in Figure 9. In this same figure, the BER values obtained for each object are also shown.

In this figure, full circles show the BER of holograms stored for the object of 300x300 bits. Notice that 71 holograms with an average BER of 0.11 have been stored. The object of 400x400 bits is depicted with empty circles in Figure 9, for which it has achieved an average BER of 0.16 for 80 multiplexed holograms. Then, the object of 500x500 bits is stored, and the BER values obtained are depicted with full squares in Figure 9. In this case, 68 holograms have been obtained with an average BER of 0.21. Finally, an object of 800x600 bits is multiplexed in the material and the corresponding BER values are depicted with empty circles in Figure 9. In this case, 72 holograms have been multiplexed with an average BER of 0.23.

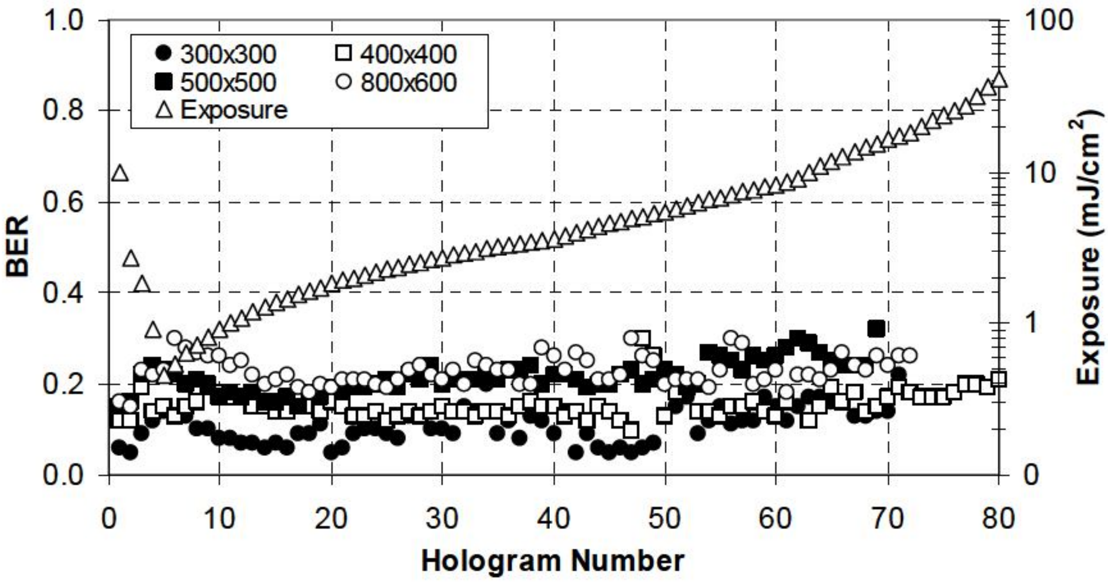

Figure 9. BER and exposure of the objects stored with the HTM configuration in a 500 μm thick material.

Finally, we will compare the results with the thickness of 500 μm for the two modulations.

For binary intensity modulation between 39 and 58 holograms with BER values close to zero have been stored. The HTM has stored between 70 and 80 holograms with BER values lower than 0.2. However, from these results we can conclude that the BER of the images increases and the image quality decreases when the number of bits in the objects increases. When the bit size is larger, the effects of blurring due to the high material thickness were not remarkable. However, when the bit size was reduced, blurring appeared in the image, decreasing its quality.

CONCLUSION

In this chapter, storage capacity of a photopolymer has been analyzed for use as a holographic memory. For this purpose, 90 diffraction gratings have been multiplexed in photopolymer layers of 700 μm thickness. Secondly, we have multiplexed data pages with different pixel sizes by using two types of object beam modulation: binary intensity modulation and hybrid ternary modulation.

The advantage of holographic storage using binary intensity modulation is that it allows image quality with very low BER values regardless of the thickness of the recording material. The disadvantages of such type of modulation are that they do not allow storage of a large number of holograms (maximum 58 holograms with a thickness of 500 μm) and that this type of storage is very sensitive to defects in the recording material.

In the case of the HTM, the main advantage is that one can store a greater number of holograms (80 to 500 μ m thick). Furthermore, such storage is not sensitive to defects in the recording material. However, it has been observed that increasing the thickness of the material gives rise to a blur in the image and increases the BER values depending on the resolution of the object.

REFERENCES

[1] Dhar, L.; Curtis, K.; Fäcke, T. *Nat. Phot*. 2008, vol. 2, 403-405.

[2] Graham-Rowe, D. *Nat. Phot*. 2007, vol. 1, 197-200.

[3] Lu, K.; Saleh, B. E. A. *Opt. Eng*. 1990, vol. 29, 240-246.

[4] Yamauchi, M.; Eiju, T. *Opt. Comm*. 1995, vol. 115, 19-25.

[5] Kim, H.; Lee, Y. H. *Appl. Opt*. 2005, vol. 44, 1642-1649.

[6] Márquez, A.; Iemmi, C.; Moreno, I.; Davis, J. A.; Campos, J.; Yzuel, M. J. *Opt. Eng*. 2001, vol. 40, 2558-2564.

[7] Marquez, A.; Gallego, S.; Mendez, D.; Alvarez, M. L.; Fernandez, E.; Ortuno, M.; Neipp, C.; Belendez, A.; Pascual, I. *Opt. Lett*. 2007, vol. 32, 2511-2513.

[8] Guerrero, R. A. Opt. Comm. 2005, vol. 245, 75-83.

[9] Joseph, J.; Waldman, D. A. *Appl. Opt*. 2006, vol. 45, 6374-6380.

[10] Remenyi, J.; Varhegyi, P.; Domjan, L.; Koppa, P.; Lorincz, E. *Appl. Opt*. 2003, vol. 42, 3428-3434.

[11] Renu, J.; Joby, J.; Kehar, S. *Opt. Laser Eng*. 2005, vol. 43, 183-194.

[12] Márquez, A.; Gallego, S.; Mendez, D.; Alvarez, M. L.; Fernández, E.; Ortuño, M.; Neipp, C.; Beléndez, A.; Pascual, I. *Opt. Lett*. 2007, vol. 32, 2511-2513.

[13] Das, B.; Vyas, S.; Joseph, J.; Senthilkumaran, P.; Singh, K. *Opt. Laser Eng*. 2009, vol. 47, 1150-1159.

[14] Das, B.; Joseph, J.; Singh, K. *Opt. Comm*. 2009, vol. 282, 2147-2154.

[15] Domjan, L.; Koppa, P.; Szarvas, G.; Remenyi, J. *Optik*, 2002, vol. 113, 382-390.

[16] Márquez, A.; Gallego, S.; Méndez, D.; Álvarez, M. L.; Fernández, E.; Ortuño, M.; Beléndez, A.; Pascual, I. In Liquid crystals and applications in optics; Glogarova, M.; PalffyMuhoray, P.; Copic, M., eds.; *Proceeding of SPIE*, US, 2007; Vol. 6587, pp 58715-58715.
[17] Jang, J. S.; Shin, D. H. *Opt. Lett*. 2001, vol. 26, 1797-1799.
[18] Ortuño, M.; Gallego, S.; García, C.; Neipp, C.; Beléndez, A.; Pascual, I. *Appl. Phys. B*. 2003, vol. 76, 851-857.
[19] Schnoes, M.; Ihas, B.; Hill, A.; Dhar, L.; Michaels, D.; Setthachayanon, S.; Schomberger, G.; Wilson, W. L. In Practical Holography XVII and Holographic Materials IX; Tung H.Jeong, ed.; *Proceeding of SPIE*, US, 2003; Vol. 5005, pp 29-37.
[20] Mcleod, R. R.; Daiber, A. J.; McDonald, M. E.; Robertson, T. L.; Slagle, T.; Sochava, S. L.; Hesselink, L. *Appl. Opt*. 2005, vol. 44, 3197-3207.
[21] Pu, A.; Psaltis, D. *Appl. Opt*. 1996, vol. 35, 2389-2398.
[22] Pu, A.; Curtis, K.; Psaltis, D. Opt. Eng. 1996, vol. 35, 2824-2829.
[23] Coufal, H.; Psaltis, D.; Sincerbox, G. T. Holographic Data Storage; Springer-Verlag: New Cork, 2000.
[24] El Hafidi, I.; Grzymala, R.; Kiefer, R.; Elouad, L.; Meyrueis, P. *Opt. Laser Technol*. 2005, vol. 37, 503-508.
[25] Curtis, K.; Pu, A.; Psaltis, D. Opt. Lett. 1994, vol. 19, 993-994.
[26] Sherif, H.; Naydenova, I.; Martin, S.; McGinn, C.; Toal, V. J. Opt. A: *Pure Appl. Opt*. 2005, vol. 7, 255-260.
[27] Rakuljic, G. A.; Leyva, V.; Yariv, A. Opt. Lett. 1992, vol. 17, 1471-1473.
[28] Cao, L. C.; Ma, X. S.; He, Q. S.; Long, H.; Wu, M. X.; Jin, G. F. *Opt. Eng*. 2004, vol. 43, 2009-2016.
[29] Bunsen, M.; Okamoto, A.; Takayama, Y. Opt. Comm. 2004, vol. 235, 41-47.
[30] Hariharan, P. Basics of Holography; Cambridge University Press: United Kingdom, 2002.
[31] Hsu, K. Y.; Lin, S. H.; Hsiao, Y. N.; Whang, W. T. *Opt. Eng*. 2003, vol. 42, 1390-1396.
[32] Kim, W. S.; Chang, H. S.; Jeong, Y. C.; Lee, Y. M.; Park, J. K.; Shin, C. W.; Nam, K.; Tak, H. J. *Opt. Comm*. 2005, vol. 249, 65-71.
[33] Barachevskii, V. A. *High Energy Chem*. 2006, vol. 40, 131-141.
[34] Ramos, G.; Álvarez-Herrero, A.; Belenguer, T.; Levy, D.; del Monte, F. In Organic Holographic Materials and Applications; Meerholz, K., ed.; *Proceeding of SPIE*, US, 2003; Vol. 5216, pp 116-126.

[35] Lin, S. H.; Chen, P. L.; Hsiao, Y. N.; Whang, W. T. *Opt. Comm*. 2008, vol. 281, 559-566.

[36] Luo, S. J.; Chen, K. X.; Cao, L. C.; Liu, G. D.; He, Q. S.; Jin, G. F.; Zeng, D. X.; Chen, Y. *Opt. Express*, 2005, vol. 13, 3123-3128.

[37] Banyal, R. K.; Prasad, B. R. *Opt. Comm*. 2007, vol. 274, 300-306.

[38] Hackel, M.; Kador, L.; Kropp, D.; Schmidt, H. W. *Adv. Mater*. 2007, vol. 19, 227.

[39] Ortuño, M.; Fernández, E.; Gallego, S.; Beléndez, A.; Pascual, I. *Opt. Express*, 2007, vol. 15, 12425-12435.

[40] Ortuño, M.; Fernández, E.; Gallego, S.; Márquez, A.; Neipp, C.; Pascual, I.; Beléndez, A. In Practical Holography Xxii: Materials and Applications; Bjelkhagen, H.; Kostuk, R., eds.; *Proceeding of SPIE*, US, 2008; Vol. 6912, pp 91207-91207.

[41] Gallego, S.; Ortuño, M.; García, C.; Neipp, C.; Beléndez, A.; Pascual, I. *J. Mod. Opt*. 2005, vol. 52, 1575-1584.

[42] Mok, F. H.; Burr, G. W.; Psaltis, D. *Opt. Lett*. 1996, vol. 21, 896-898.

[43] Yan, A. Q.; Tao, S. Q.; Wang, D. Y.; Shi, M. Q.; Wu, F. P. In Advances in optical data storage technology; Duanyi Xu; Kees A.Schouhamer Immink; Keiji Shono, eds.; *Proceeding of SPIE*, US, 2005; Vol. 5643, pp 109-117.

[44] Murciano, A.; Blaya, S.; Carretero, L.; Ulibarrena, M.; Fimia, A. *Appl. Phys. B*. 2005, vol. 81, 167-169.

[45] Fernández, E.; García, C.; Pascual, I.; Ortuño, M.; Gallego, S.; Beléndez, A. *Appl. Opt*. 2006, vol. 45, 7661-7666.

[46] Fernández, E.; Ortuño, M.; Gallego, S.; García, C.; Beléndez, A.; Pascual, I. *Appl. Opt*. 2007, vol. 46, 5368-5373.

[47] Fernández, E.; Ortuño, M.; Márquez, A.; Gallego, S.; Pascual, I. In Photon Management Ii; Sheridan, J. T.; Wyrowski, F., eds.; *Proceeding of SPIE*, US, 2006; Vol. 6187, pp U391-U397.

[48] Durán, V.; Lancis, J.; Tajahuerce, E.; Jaroszewicz, Z. J. *Appl. Phys*. 2005, vol. 97, 043101/1-043101/6.

[49] Márquez, A.; Iemmi, C.; Campos, J.; Yzuel, M. J. *Opt. Lett*. 2006, vol. 31, 392-394.

[50] Fernández, E.; Ortuño, M.; Gallego, S.; García, C.; Márquez, A.; Beléndez, A.; Pascual, I. In Practical Holography Xxii: Materials and Applications; Bjelkhagen, H.; Kostuk, R., eds.; *Proceeding of SPIE*, US, 2008; Vol. 6912, pp 91214.

[51] Márquez, A.; Campos, J.; Yzuel, M. J.; Moreno, I.; Davis, J. A.; Iemmi, C. *Opt. Eng*. 2000, vol. 39, 3301-3307.

[52] Soutar, C.; Lu, K. *Opt. Eng*. 1994, vol. 33, 2704-2712.
[53] Davis, J. A.; Allison, D. B.; D'Nelly, K. G.; Wilson, M. L.; Moreno, I. *Opt. Eng*. 1999, vol. 38, 705-709.
[54] Fernández, E.; Ortuño, M.; Gallego, S.; Márquez, A.; García, C.; Beléndez, A.; Pascual, I. *Appl. Opt*. 2008, vol. 47, 4448-4456.
[55] Fernández, E.; Ortuño, M.; Gallego, S.; Márquez, A.; García, C.; Fuentes, R.; Beléndez, A.; Pascual, I. *Optik*, 2010, vol. 121, 151-158.
[56] Fernández, E.; Márquez, A.; Gallego, S.; Fuentes, R.; García, C.; Pascual, I. J. *Lightwave Technol*. 2010, vol. 28, 776-783.